Optics Letters

Femtosecond pulse generation from a Ti^{3+}: sapphire laser near 800 nm with voltage reconfigurable graphene saturable absorbers

Isinsu Baylam,[1] Sarper Ozharar,[2] Nurbek Kakenov,[3] Coskun Kocabas,[3] and Alphan Sennaroglu[1,4,*]

[1]Laser Research Laboratory, Departments of Physics and Electrical-Electronics Engineering, Koç University, Istanbul 34450, Turkey
[2]College of Engineering and Natural Sciences, Department of Electrical-Electronics Engineering, Bahçeşehir University, Beşiktaş, Istanbul 34353, Turkey
[3]Department of Physics, Bilkent University, Ankara 06800, Turkey
[4]Koç University Surface Science and Technology Center (KUYTAM), Koç University, Istanbul 34450, Turkey
*Corresponding author: asennar@ku.edu.tr

Received 23 November 2016; accepted 2 March 2017; posted 13 March 2017 (Doc. ID 281433); published 30 March 2017

We experimentally show that a voltage-controlled graphene-gold supercapacitor saturable absorber (VCG-gold-SA) can be operated as a fast saturable absorber with adjustable linear absorption at wavelengths as low as 795 nm. This was made possible by the use of a novel supercapacitor architecture, consisting of a high-dielectric electrolyte sandwiched between a graphene and a gold electrode. The high-dielectric electrolyte allowed continuous, reversible adjustment of the Fermi level and, hence, the optical loss of the VCG-gold-SA up to the visible wavelengths at low bias voltages of the order of a few volts (0–2 V). The fast saturable absorber action of the VCG-gold-SA and the bias-dependent reduction of its loss were successfully demonstrated inside a femtosecond Ti^{3+}:sapphire laser operating near 800 nm. Dispersion compensation was employed by using dispersion control mirrors and a prism pair. At a bias voltage of 1.2 V, the laser operated with improved power performance in comparison with that at zero bias, and the VCG-gold-SA initiated the generation of nearly transform-limited pulses as short as 48 fs at a pulse repetition rate of 131.7 MHz near 830 nm. To the best of our knowledge, this represents the shortest wavelength where a VCG-gold-SA has been employed as a mode locker with adjustable loss.

OCIS codes: (140.4050) Mode-locked lasers; (140.7090) Ultrafast lasers; (160.4236) Nanomaterials; (140.5680) Rare earth and transition metal solid-state lasers.

https://doi.org/10.1364/OL.42.001404

Due to its ultrabroadband saturable absorption and ultrafast relaxation, monolayer graphene has been successfully employed as a saturable absorber in lasers operating at different wavelength ranges [1–3]. However, one potential drawback arises because even a monolayer graphene has a single-pass, small-signal absorption of 2.3%, and this can lead to excessive insertion losses, especially in low-gain lasers or in lasers operated at low pumping levels. This limitation can be obviated by using gated graphene structures to vary the Fermi level and, hence, the total absorption, while maintaining a sufficient level of saturation to initiate mode-locked operation [4–6]. One example involves the use of solid-state graphene capacitors. Such devices can be used for controlling the absorption level of graphene, but they typically require high operating voltages and face the risk of dielectric breakdown [7,8]. Chemical doping of graphene offers an alternative approach to shift the Fermi level but, in this case, the shift is fixed and cannot be dynamically controlled [9].

In our recent experiments, we have proposed and demonstrated novel graphene supercapacitor architectures that provide reversible control of the loss level at low bias voltages and which can, at the same time, initiate femtosecond pulse generation from lasers [4–6]. The preliminary design consisted of two graphene electrodes separated by an electrolyte with a high dielectric constant [4]. To further reduce the insertion losses at zero bias, we developed a second, more versatile supercapacitor device composed of the same electrolyte sandwiched between a graphene electrode and a notched gold electrode [5]. We will refer to this voltage reconfigurable device as the voltage-controlled graphene-gold saturable absorber or, shortly, VCG-gold-SA. Our experiments showed that VCG-gold-SA enabled superior power and mode-locking performance at lower operating voltages, in comparison with the supercapacitor saturable absorber consisting of two graphene electrodes. The design of the VCG-gold-SA is unique since its insertion loss can, in principle, be reduced below that of a monolayer graphene, provided that the losses arising from the substrate and the electrolyte are negligible. To demonstrate the mode-locking performance of our supercapacitor devices, we used a multipass-cavity Cr^{4+}:forsterite laser and obtained sub-100 fs pulses near 1250 nm [4,5]. Other studies employed a different supercapacitor architecture to modulate a fiber laser near 1.6 μm [10]. With regard to VCG-gold-SAs, the next challenge involves pushing the modulation capability to as low a wavelength as possible. The difficulty here arises because

of the fact that as the operation wavelength is lowered; a larger bias voltage is needed to vary the loss of the device via Pauli blocking, leading to a higher risk of dielectric breakdown. In this Letter, to the best of our knowledge, we describe the first successful operation of a VCG-gold-SA in the 800 nm wavelength region. The fast saturable absorber action of the VCG-gold-SA and the bias-dependent reduction of its loss were successfully demonstrated by using a Ti^{3+}:sapphire laser operating near 830 nm. In the mode-locking experiments, two different types of dispersion control based on a prism pair and dispersion control mirrors (DCMs) were further investigated. At a bias voltage of 1.2 V, the laser operated with improved power performance in comparison with that at zero bias, and the VCG-gold-SA initiated the generation of nearly transform-limited pulses as short as 48 fs at a pulse repetition rate of 131.7 MHz near 830 nm. To the best of our knowledge, this represents the shortest wavelength where a VCG-gold-SA has been employed as a mode locker with adjustable loss.

Mode-locking performance and bias-dependent loss of the VCG-gold-SA were tested by using a home-built *x*-cavity Ti^{3+}:sapphire laser operating near 830 nm. As can be seen from the sketch of the experimental setup in Fig. 1, the laser cavity contained a Brewster-cut, 2.3 mm long Ti^{3+}:sapphire crystal (pump absorption = 74% at 532 nm), positioned between two curved high reflectors [HRs] (C1 and C2), each with a radius of curvature of 50 mm. The cavity further contained a flat end HR, a flat 3% transmitting output coupler (OC), and a second pair of curved HRs (C3 and C4, radius of *c* urvature = 150 mm) between which the VCG-gold-SA was positioned. An input lens (L) with a focal length of 50 mm was used to focus the pump beam inside the crystal to an estimated waist of 17 μm. During the experiments, the Ti^{3+}:sapphire crystal was held inside a copper holder and kept at a constant temperature of 20°C by water cooling. The VCG-gold-SA used in the experiments consisted of a graphene electrode and a notched gold electrode (diameter = 5 mm) with an ionic liquid electrolyte (diethymethyl (2-methoxyethyl) ammonium bis (trifluro-methylsulfony) imide [DEME] [TFSI]) sandwiched between the electrodes. This specific electrolyte had a high optical transmission around 800 nm, and its relative dielectric constant ($\epsilon_r = 14$) was high enough to avoid dielectric breakdown when the device was modulated up to visible wavelengths. The VCG-gold-SA was the same device employed in our previous study conducted near 1250 nm, and the detailed fabrication scheme can be found in [5]. During the mode-locking experiments, the VCG-gold-SA was placed at Brewster incidence near the beam waist location between C3 and C4 (see Fig. 1) to minimize reflection losses and to maximize the light fluence on the device. For the Ti^{3+}:sapphire cavity shown in Fig. 1, the estimated beam waist on the VCG-gold-SA and the pulse repetition rate of the composite cavity were 65 μm and 131.7 MHz, respectively. Two different

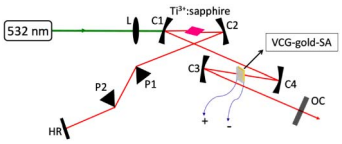

Fig. 1. Sketch of the Ti^{3+}:sapphire laser, mode locked with the voltage-controlled graphene-gold saturable absorber (VCG-gold-SA).

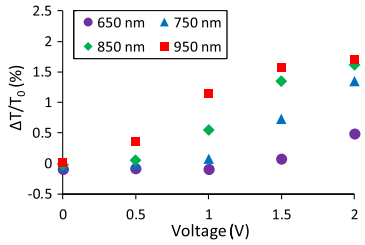

Fig. 2. Measured fractional change in the optical transmission of the VCG-gold-SA at normal incidence as a function of the applied voltage at four selected wavelengths.

dispersion control schemes were employed during the mode-locking experiments to balance the Kerr nonlinearities and to compensate for the positive dispersion due to the Ti^{3+}:sapphire crystal, air, and other intracavity elements. In the first case, only DCMs were added to the resonator. Here, the net round-trip group delay dispersion (GDD) of the laser was estimated to be −248 fs^2. In the second case, a combination of DCMs (HR, C1, and C2) and a pair of SF-14 prisms (P1 and P2 in Fig. 1) with a tip-to-tip separation of 13 cm were used. In this case, by taking into account the additional negative GDD due to C1, C2, and HR (−50 fs^2 for C1 and C2, −40 fs^2 for HR), the net round-trip GDD of the composite resonator was estimated to be −182 fs^2. The optimum mode-locking performance was obtained with the composite laser resonator containing the SF-14 prism pair which allowed a finer adjustment of cavity GDD and led to the generation of shorter pulses as discussed in the next section.

Before the mode-locking experiments, we first investigated the voltage-dependent transmission of the VCG-gold-SA. Figure 2 shows the measured fractional change in the optical transmission ($\Delta T/T_0$, ΔT = bias-dependent change in the transmission, T_0 = transmission at zero bias) of the VCG-gold-SA at normal incidence as a function of the applied voltage at four wavelengths.

As can be seen, by applying bias voltages as low as 2 V, a fractional transmission change of nearly 0.5% could be achieved at 650 nm, clearly demonstrating the low-voltage modulation capability of the device. Near the operation wavelength of our laser (850 nm), a bias voltage of 1 V was sufficient to obtain the same fractional change in transmission. This is because, as the wavelength decreases, the photon energy increases, and a larger bias voltage is required to reduce the absorption via Pauli blocking. Reference [5] provides a more complete set of voltage-dependent optical transmission spectra for our device.

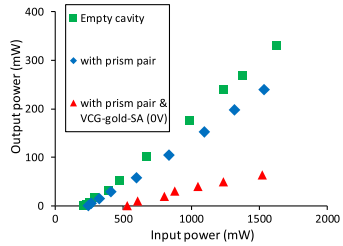

Fig. 3. Continuous-wave power performance of the Ti^{3+}:sapphire laser with the 3% OC in different cavity configurations.

Figure 3 shows the continuous-wave power performance of the Ti^{3+}:sapphire laser with different cavity configurations. The resonator consisting of the crystal, curved cavity mirrors (C1, C2, C3, and C4), end HR, and the 3% OC, was operated with a power slope efficiency of 23.5%. The threshold pump power was 212 mW. After introducing the prism pair, the measured slope efficiency decreased to 18.5%, and the threshold pump power increased to 245 mW. The VCG-gold-SA was positioned between the curved HRs C3 and C4, as shown in Fig. 1, resulting in a further increase in the threshold pump power (533 mW) and a decrease in the slope efficiency (6.4%) for the composite cavity at zero bias. However, the application of a bias voltage to the VCG-gold-SA readily led to an increase in the output power of the Ti^{3+}:sapphire laser from 58 to 113 mW [see Fig. 4(a), input pump power = 1.6 W]. The corresponding single-pass insertion loss of the device was further investigated by measuring the threshold pump power at different bias voltages and performing a similar analysis, as described in Refs. [5,11].

Figure 4(b) shows the measured single-pass insertion loss of the VCG-gold-SA as a function of the bias voltage. We were able to reduce the single-pass insertion loss of the device from 4.3% to 1.3% at the photon energy of 1.49 eV (830 nm) without encountering dielectric breakdown. For bias voltages above 0.5 V, the insertion loss of the device decreased due to Pauli blocking and, for voltages greater than 1.5 V, the absorption of the graphene electrode was completely blocked. Hence, for bias voltages above 1.5 V, the graphene electrode becomes transparent at 830 nm, and the remaining losses were due to the substrates and the electrolyte. As a result of the electrostatic doping arising from the ultrathin electrical double layer formation on both electrodes, the electric field was generated only within the double layers, leaving the bulk of the electrolyte neutral. Hence, the 5 mm notch or the thickness of the ionic liquid did not have a profound influence on the device operation. This was tested by measuring the output power of the laser at the bias voltage of 1.5 V by translating the supercapacitor across the notch. As shown in Fig. 4(c), the response of the device was nearly the same across the 5 mm notch, except near one of the edges.

Once the OC was translated, the VCG-gold-SA readily enabled the initiation of single-pulse mode-locked operation of the Ti^{3+}:sapphire laser at low bias voltages. At first, only

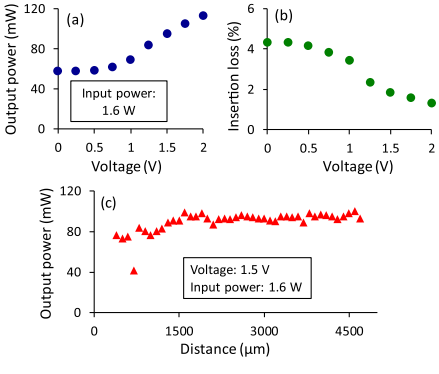

Fig. 4. (a) Measured laser output power as a function of the applied bias at a fixed input pump power of 1.6 W. (b) Measured change in the single-pass insertion loss of the VCG-gold-SA as a function of the bias voltage. (c) Output power of the laser at the bias voltage of 1.5 V, measured by translating the supercapacitor across the 5 mm notch.

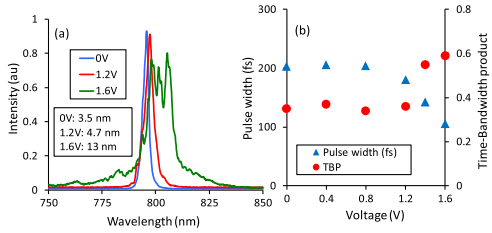

Fig. 5. (a) Mode-locked output spectra obtained at different bias voltages in the cavity configuration employing DCMs. (b) Corresponding voltage-dependent pulse durations and time-bandwidth products as a function of the bias voltage.

DCMs were used for dispersion compensation. In this case, the net GDD of the cavity was estimated to be −248 fs^2. Figure 5(a) shows the mode-locked spectra obtained in this case at three different bias levels of 0, 1.2, and 1.6 V. The laser center wavelength was around 800 nm with spectral widths [full-width half-maximum (FWHM)] of about 3.5–4.5 nm for bias voltages less than 1.2 V. At the bias voltage of 1.2 V, we obtained the largest spectral width of 4.7 nm (FWHM) while the output pulses remained nearly transform limited (pulse duration of 180 fs). Since the net GDD was fixed in the DCM configuration, higher applied voltages resulted in lower cavity loss and higher intracavity energies, leading to larger spectral widths and shorter pulse durations. However, as shown in Figs. 5(a) and 5(b), at voltages greater than 1.2 V, the mode-locked bandwidths increased and the pulses became chirped with time-bandwidth products increasing to around 0.6, possibly due to the GDD oscillations of the DCMs.

Hence, in order to provide adjustable dispersion and to reduce GDD oscillations, 3 DCMs were removed from the cavity, and a pair of SF-14 prisms was added, as shown in Fig. 1. For this configuration, at the bias voltage of 0 V, the composite resonator operating around 830 nm produced 62 fs pulses with a time-bandwidth product of 0.35 at an output power of 55 mW. By increasing the applied voltage up to 1.2 V, we were able to increase the intracavity energy of the Ti^{3+}:sapphire resonator and reduce the pulse duration to 48 fs (time-bandwidth product = 0.37).

Figure 6 shows the mode-locking results obtained at 1.2 V of applied bias. The autocorrelation trace and the mode-locked spectrum for the 48 fs pulses are shown in Figs. 6(a) and 6(b), respectively (output power = 76 mW). Figure 6(c) further shows that at the pulse repetition rate of 131.7 MHz, the radio

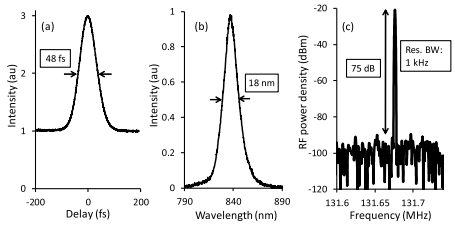

Fig. 6. (a) Intensity autocorrelation trace, (b) mode-locked optical spectrum, and (c) RF spectrum of the mode-locked pulses initiated with the VCG-gold-SA at the bias voltage of 1.2 V. The prism pair was used for dispersion compensation.

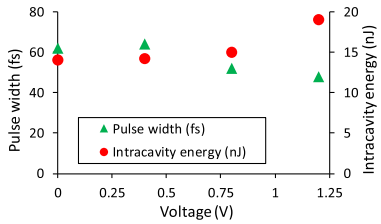

Fig. 7. Measured pulse durations and the corresponding intracavity pulse energies as a function of the applied bias for the Ti^{3+}:sapphire laser mode locked with the VCG-gold-SA. The OC transmission was 3%.

frequency (RF) spectrum of the fundamental beat note was at least 75 dB above the carrier level, indicating a stable mode-locked operation. At the bias voltage of 1.2 V, the maximum incident fluence on the VCG-gold-SA was estimated to be 143 $\mu J/cm^2$ and no damage was observed on the device up to this fluence level.

For the setup with the prism pair, we further explored the voltage-dependent pulse characteristics by measuring the pulse duration and the corresponding intracavity energy as a function of the applied bias during single-pulse mode-locked operation.

The data are shown in Fig. 7. As expected from the soliton-area theorem [12], as the bias voltage was increased, the intracavity energy increased and the resulting pulse duration decreased from 62 fs to 48 fs. In the 0–1.2 V range of bias voltages, the pulses remained nearly transform limited with time-bandwidth products between 0.33 and 0.37. For voltages greater than 1.2 V, mode-locked operation at 830 nm could not be obtained as a result of the Pauli blocking. The total round-trip GDD due to the VCG-gold-SA, cavity optics, and the prism pair was estimated to be $-182\ fs^2$. We further calculated the total net GDD of the resonator by using the nonlinear refractive index of Ti^{3+}:sapphire [13] and the soliton-area theorem which relates the pulse width to the intracavity energy [12]. The GDD level, calculated from the soliton-area theorem came to $-184\ fs^2$, in good agreement with the estimated value.

For both the DCM and prism-pair configurations, we were able to experimentally verify that mode-locking was initiated by the fast saturable absorber action of the VCG-gold-SA and not by Kerr-lens mode locking (KLM). To verify this, the OC was translated to initiate mode locking at different bias voltages. For the DCM configuration, mode-locked operation could not be initiated at bias voltages beyond 1.6 V because fast saturable absorption in the device would vanish at greater voltages due to Pauli blocking. Had KLM been the initiation mechanism, pulse generation would have started irrespective of the bias voltage applied to the VCG-gold-SA. In the case of the prism pair, mode-locked operation could not be initiated for voltages greater than 1.2 V. We believe that the difference could be due to somewhat different levels of loss introduced by the different dispersion compensation schemes or due to the degradation in operation of the device over several months with a bias voltage near 2 V, which is close to the electrochemical window of the electrolyte. In our previous experiments conducted around 1.25 μm, we did not encounter this behavior since the device was operated at voltages less than 1 V.

In conclusion, we have successfully employed a voltage-controlled graphene-gold saturable absorber (VCG-gold-SA) to initiate mode-locked operation of a Ti^{3+}:sapphire laser at 830 nm. By varying the applied bias from 0 V to 2 V, the insertion loss of the VCG-gold-SA could be decreased from 4.3% to 1.3%. At a bias voltage of 1.2 V, nearly transform limited, 48 fs pulses could be generated near 830 nm. To the best of our knowledge, this is the shortest wavelength where the VCG-gold-SA has been employed as a fast saturable absorber. We note that the same device with voltage-dependent insertion loss was previously used to generate femtosecond pulses from a Cr^{4+}:forsterite laser operating near 1.25 μm [5]. Based on the results of this Letter and the previous experiments conducted at 1.25 μm, we believe that the VCG-gold-SA has the potential to become a versatile fast saturable absorber which is suitable for the mode locking of lasers operating at different wavelengths and with different levels of gain.

Funding. Türkiye Bilimsel ve Teknolojik Arastirma Kurumu (TÜBITAK) (113F278).

Acknowledgment. The authors thank Abdullah Muti and Can Cihan for their help during the experiments.

REFERENCES

1. I. H. Baek, H. W. Lee, S. Bae, B. H. Hong, Y. H. Ahn, D.-I. Yeom, and F. Rotermund, Appl. Phys. Express **5**, 032701 (2012).
2. M. N. Cizmeciyan, J. W. Kim, S. Bae, B. H. Hong, F. Rotermund, and A. Sennaroglu, Opt. Lett. **38**, 341 (2013).
3. Z. Sun, T. Hasan, and A. C. Ferrari, Physica E **44**, 1082 (2012).
4. I. Baylam, M. N. Cizmeciyan, S. Ozharar, E. O. Polat, C. Kocabas, and A. Sennaroglu, Opt. Lett. **39**, 5180 (2014).
5. I. Baylam, O. Balci, N. Kakenov, C. Kocabas, and A. Sennaroglu, Opt. Lett. **41**, 910 (2016).
6. E. O. Polat and C. Kocabas, Nano Lett. **13**, 5851 (2013).
7. C. C. Lee, C. Mohr, J. Bethge, S. Suzuki, M. E. Fermann, I. Hartl, and T. R. Schibli, Opt. Lett. **37**, 3084 (2012).
8. C. C. Lee, S. Suzuki, W. Xie, and T. R. Schibli, Opt. Express **20**, 5264 (2012).
9. H. T. Liu, Y. Q. Liu, and D. B. Zhu, J. Mater. Chem. **21**, 3335 (2011).
10. E. J. Lee, S. Y. Choi, H. Jeong, N. H. Park, W. Yim, M. H. Kim, J. K. Park, S. Son, S. Bae, S. J. Kim, K. Lee, Y. H. Ahn, K. J. Ahn, B. H. Hong, J. Y. Park, F. Rotermund, and D. I. Yeom, Nat. Commun. **6**, 6851 (2015).
11. S. Ozharar, I. Baylam, M. N. Cizmeciyan, O. Balci, E. Pince, C. Kocabas, and A. Sennaroglu, J. Opt. Soc. Am. B **30**, 1270 (2013).
12. H. A. Haus, IEEE J. Sel. Top. Quantum Electron. **6**, 1173 (2000).
13. E. Sorokin, *Few-Cycle Laser Pulse Generation and Its Applications*, F. X. Kartner, ed. (Springer, 2004), pp. 3–71.